DOI: 10.61782/fa.2023.1114

forum acusticum 2023

UNCERTAINTY OF INPUT DATA FOR WAVE-BASED ROOM ACOUSTIC SIMULATIONS IN LARGE NON-TRIVIAL ENVIRONMENTS

Giulia Fratoni* **Dario D'Orazio** **Massimo Garai**
Department of Industrial Engineering (DIN), University of Bologna, Italy

ABSTRACT

In the last decades, wave-based simulation methods have been applied to an increasing number of 3D virtual rooms thanks to the scientific and computational advances in numerical models. However, there is still a lack of adequate material properties required for those simulations, in terms of accessible lists of various frequency-dependent boundary conditions. Such input parameters can be retrieved from sound absorption coefficients, exploiting the availability of several consolidated datasets typically employed in ray-tracing simulations. The present work aims at quantifying and assessing the degree of uncertainty underlying this critical step in non-trivial environments. With this purpose, parallel calibrations have been carried out on distinct case studies based on experimental data using finite-difference time-domain (FDTD) and geometrical acoustics (GA) approaches. The outcomes highlight significant discrepancies at low frequencies between the different input data for various materials, suggesting a potential decrease (up to 45%) in sound absorption coefficient before the conversion to specific acoustic impedances.

Keywords: *room acoustic simulations, finite-difference time-domain, wave-based methods, boundary conditions*

1. INTRODUCTION

The reliability of boundary conditions is crucial to achieve accurate results in room acoustic simulations. In scientific literature, most of the available datasets are energy-based quantities, i.e., sound absorption coefficients, for various reasons. First, the geometrical acoustics (GA) approach has historically been the main tool to simulate the acoustic field in large enclosed spaces, requiring energy-based input data as material properties [1–3]. Secondly, methods adopted by the ISO 354 standard and the ASTM C423 are the most widespread procedures to measure the frequency-dependent randomly-incident absorption coefficients in third octave bands [4, 5]. This led to collect a wide number of consolidated absorption coefficient datasets that are available for engineers, architects, acousticians, and scholars [6, 7].

In the last decades, also wave-based (WB) methods have been widely applied to acoustic simulations [8, 9]. In fact, technological advances in parallel computation through GPUs allowed a wide use of optimized WB codes in room acoustics, partially overcoming the inherent disadvantages related to high computational cost, which typically increases with frequency and with the size of the room [10–12]. Nevertheless, even though WB simulations have gained an important role in the room acoustic research field, there is still a certain lack of proper input data, i.e., pressure-based quantities, such as complex acoustic impedances or reflection factors. Consequently, a common practice adopted in WB models is to exploit the wide availability of absorption coefficients converting these energy-based quantities into acoustic impedances [13, 14]. However, this retrieval process yields to non-unique solutions because there are infinite surface impedance values corresponding to a certain value of absorption coefficient [15]. Moreover, when time-dependent approaches are adopted, such as the discontinuous Galerkin method and the finite-difference time-domain method, time-dependent boundary conditions are needed [16, 17].

The present work explores the uncertainty of such conversion process in large non-trivial geometries, using finite-difference time-domain (FDTD) models [18]. In

**Corresponding author*: giulia.fratoni2@unibo.it.

parallel, GA calibration of the same 3D models allowed to outline a comparison between the different boundary conditions employed [19].

2. BACKGROUND THEORY

Given a boundary hit by a sound wave, the complex reflection factor is the ratio between the reflected pressure and the incident pressure $R = p_{refl}/p_{in} = |R|e^{i\chi}$ where $|R|$ is the magnitude and χ the phase of the reflected sound wave. The reflection factor completely describes the angle-dependent and frequency-dependent acoustic properties of a surface. As the intensity of a plane wave is proportional to the square of the pressure amplitude ($I = p^2/\rho_0 c$), the fraction of intensity of the reflected wave is reduced proportionally to a quantity equal to $|R|^2$ with respect to the total energy of the incident sound wave. Therefore, for plane waves incident on infinite surfaces, the quantity $1 - |R|^2$ indicates the fraction of intensity lost during the reflection, which is defined as the absorption coefficient α:

$$\alpha = 1 - |R|^2. \tag{1}$$

The acoustic properties of a surface can also be described with the complex specific acoustic impedance, which is the ratio between the sound pressure at the surface and the normal component of the particle velocity at the incidence point:

$$Z = \frac{p}{v_n} \quad \text{(rayl)}. \tag{2}$$

The normalized specific acoustic impedance is expressed as $\zeta = Z/\rho_0 c_0$ where $\rho_0 c_0$ is the characteristic acoustic impedance of the air ($\simeq 415\,\mathrm{kg/m^2 s}$ at 20° C), whilst its inverse value is defined as the admittance $\gamma = 1/\zeta$ [15]. In case of normal-incident wave ($\theta = 0$):

$$R = \frac{Z_s - Z_0}{Z_s + Z_0} = \frac{\zeta - 1}{\zeta + 1} \tag{3}$$

and consequently:

$$\alpha(\zeta) = \frac{4\mathrm{Re}(\zeta)}{|\zeta|^2 + 2\mathrm{Re}(\zeta) + 1}. \tag{4}$$

Notwithstanding the inherent uncertainty when transforming absorption coefficients into surface impedances, scholars agree on the combined use of input absorption coefficients and the absorber category of interest, such as microperforated panels, porous absorbers, and membranes. This allows to match the input absorption coefficients with existing adequate surface impedance models to obtain the most likely surface impedance based on the model [14]. . Generally, the optimization problem is expressed as:

$$F(\zeta) = |\alpha_{\gamma eq} - \alpha_{input}|^2 \tag{5}$$

where $F(\zeta)$ is the optimization function, $\alpha_{\gamma eq}$ is the absorption coefficient corresponding to ζ, and α_{input} is the Sabine absorption coefficient provided as input data. The goal is to minimize the optimization function using the constraints given from the analytical model corresponding to the type of absorber assessed [13]. In other words, conversion processes identify the type of absorber and generate the most plausible surface impedance based on such information. Basically, the start-of-art knowledge is the basis of material conversion processes. Consequently, innovative or non-trivial materials with specific acoustic properties still lack of proper models suited to the retrieving process. This issue becomes even more challenging in scenarios such as virtual models of opera houses, when the surfaces constituing the boxes tiers are generally merged into a single macro-layer with proper acoustic properties [20]. Similarly, a further example is the group of flat surfaces corresponding to the seats rows, typically with a 80 centimeters high box on the floor [21].

3. METHOD

3.1 Large non-trivial environments

With the aim of assessing challenging material properties for WB simulations, the present study explores a sample of four large opera houses, whose ISO 3382-1 room criteria had been measured through several acoustic surveys by the authors [22]. The authors acquired impulse responses using exponential sine sweep (ESS) signals. In compliance with the Ferrara Charter procedure, at least two points were selected for the omnidirectional sound sources (proscenium and centre stage), and a dense mesh of receivers was arranged throughout half of the audience areas (stalls, theatre boxes, galleries) [23]. The halls under study are different in size, occupancy, acoustic typology, acoustic coupling effects and sound absorption distribution [24–26]. For more information on the halls see [27–29].

The 3D models of the opera houses were built with Sketchup Pro according to the state-of-art acoustic modeling procedure [30,31]. During the modeling process, the choice was to reduce the actual numbers of distinct materials present in the actual opera house to a relative small

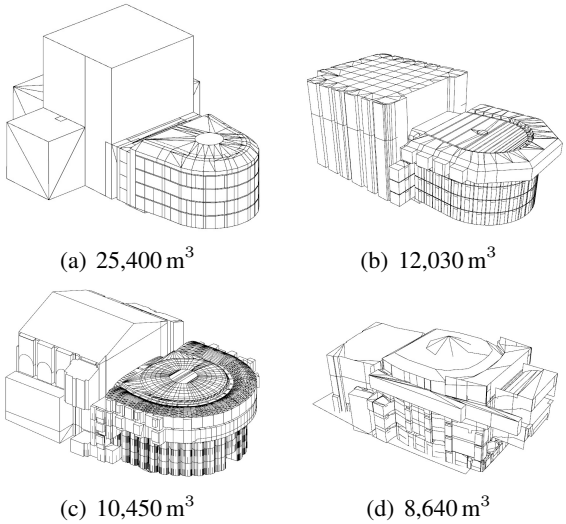

(a) 25,400 m^3 (b) 12,030 m^3

(c) 10,450 m^3 (d) 8,640 m^3

Figure 1: 3D models of large non-trivial halls under study. The total volume is provided in cubic meters.

number of layers. This contributes to minimize the uncertainty connected with the input data, as the material properties to be assigned to the surfaces [32,33]. The results of the 3D modeling phase are shown in Figure 1, along with the total volume of each hall in cubic meters.

3.2 Finite-difference time-domain models

The WB code employed in this study is a FDTD algorithm with a finite volume optimization at the boundaries developed by a group of researchers at the University of Edinburgh [34–36]. The whole hybrid code combines the FDTD/FVTD model up to a certain cut-off frequency (4 kHz) with a classical stochastic ray-tracing at high density at higher frequencies. In the FDTD part of the code, a non-Cartesian 13-point stencil cubic close-packed (CCP) scheme was used over a face-centered cubic (FCC) subgrid to minimize the dispersion errors [37]. The boundary conditions employed in the FDTD part of the code are the locally reactive complex-admittances $\gamma(\mathbf{x}, s)$, whose general expression is

$$\gamma(\mathbf{x}, s)p(\mathbf{x}, s) = \mathbf{n} \cdot \mathbf{v}(\mathbf{x}, s) \tag{6}$$

where $p(\mathbf{x}, s)$ is the sound pressure, $\mathbf{n} \cdot \mathbf{v}(\mathbf{x}, s)$ is the normal velocity component at the boundary, and s is the usual transform variable. The impulse response length was cautelatively set equal to 3 seconds to account even for the longer reverberation time values at low frequencies. Notwithstanding the significant computational cost - due to the size of the halls and the high value of the cut-off frequency - the calculation employed only 1 hour for each second of impulse response parallelizing CUDA across next-generation GPUs.

3.3 Retrieving process

The procedure employed in the present study is presented in Figure 2. First, the outcomes of the acoustic measurements have been the reference point in a standard GA calibration of the 3D models through a hybrid ray-tracing software (Odeon Room Acoustics) [38]. The sound absorption and scattering coefficients applied to the surfaces were first taken from available databases [6,7,39,40], and then adjusted in an iterative way to achieve the calibration, according to the common practice [41,42].

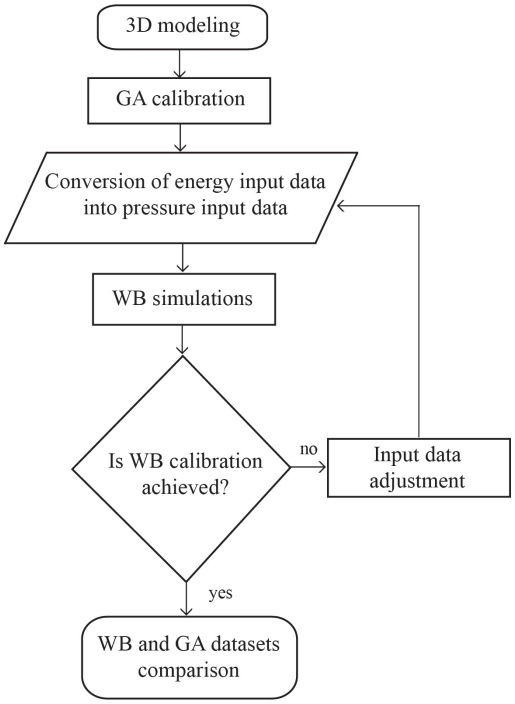

Figure 2: FDTD calibration process carried out in each of the 3D virtual models, taking the measurements as a reference point and the parallel GA calibration as a term of comparison.

Successively, the same 3D models have been tuned to the experimental data also with the FDTD approach. It is

important to remark that even though a WB model could support more details, the choice to use the same models allows a systematic comparison between FDTD and GA input dataset. In other words, the goal is maintaining comparable all the steps of the two different procedures and to carry out analyses on the final results, with a special focus on the different input datasets employed. Moreover, the choice was to start the FDTD calibration with the final energy-based quantities outcoming from the GA calibration and to derive the corresponding complex acoustic admittances, notwithstanding the non-univocity of the solution [13, 14].

In this work, boundary impedance conditions were derived from the energy parameters employed in GA calibrations using the electrical–acoustical analogy thoroughly described in [43]. The electrical–acoustical analogy with a parallel network of resistance - inductance - capacitance (RLC) circuits is employed as a one-port structure, as follows:

$$\gamma(\mathbf{x}, s) = \sum_{m=1}^{M} \frac{s}{L^{(m)}(\mathbf{x})s^2 + R^{(m)}(\mathbf{x})s + \frac{1}{C^{(m)}(\mathbf{x})}} \quad (7)$$

where $\gamma(\mathbf{x}, s)$ is the complex admittance, L, R, C are, respectively, the real-valued non-negative inductance, resistance, and capacitance of the circuit, and M is the number of different branches involved in the circuit.

4. RESULTS

The present section summarizes the calibration results and the corresponding final input data used as boundary conditions for FDTD and GA models. During the iterative process of input data adjustment for FDTD calibrations, changes have been applied to those materials whose α_{GA} are expected to be mostly affected by uncertainties, while maintaining the acoustic properties of standard materials [32, 44]. For instance, instead of changing data of surfaces related to marble, curtains, and plaster, the boundary conditions of merged or simplified materials, such as the theatre boxes or the seats rows, had been changed [21, 45].

With reference to the workflow summarized in Figure 2, FDTD calibration was achieved when simulated room criteria converged to the measured ones in all the octave bands of interest (from 125 to 4000 Hz) considering the just noticeable difference (JNDs) of each room criteria as tolerance ranges [46]. Calibration outcomes are provided in Table 1, both for FDTD and GA processes, in terms of main ISO 3382-1 room criteria at mid frequencies (500 – 1000 Hz). In detail, considering the sound source at the centre of each stage and the receivers spread throughout half of the whole audience area, measured and simulated $T_{30,\mathrm{M}}$, EDT_{M}, $C_{80,\mathrm{M}}$, and $T_{\mathrm{S,M}}$ are provided.

Table 1: Summary of GA and FDTD calibrations against measurements: the sound source is placed at the centre of each stage and the receivers are spread throughout half of the audience areas. Measured and simulated $T_{30,\mathrm{M}}$, EDT_{M}, $C_{80,\mathrm{M}}$, and $T_{\mathrm{S,M}}$ room criteria are averaged over 500 and 1000 Hz octave bands.

		$T_{30,M}$ (s)	EDT_{M} (s)	$C_{80,\mathrm{M}}$ (dB)	$T_{\mathrm{S,M}}$ (ms)
a	Meas.	1.57	1.54	0.1	119
	GA	1.65	1.53	0.6	109
	FDTD	1.56	1.43	0.1	110
b	Meas.	1.59	1.20	3.5	75
	GA	1.71	1.27	3.8	74
	FDTD	1.60	1.27	3.0	81
c	Meas.	1.39	1.12	3.7	73
	GA	1.33	1.21	4.3	69
	FDTD	1.38	1.17	3.4	78
d	Meas.	1.41	1.17	3.6	77
	GA	1.43	1.20	3.2	78
	FDTD	1.44	1.20	3.8	76

Concerning the boundary conditions at the end of the double calibration process, significant discrepancies were found for the macro-layers corresponding to theatre boxes and seat rows [18]. Figure 3 shows the comparison between FDTD and GA boundary conditions referring to the two macro-layers assessed: α_{GA} are the energy parameters actually assigned to the surfaces while $\alpha_{\gamma eq}$ have been re-converted from the acoustic admittances actually used in the simulation. It is possible to notice that $\alpha_{\gamma eq}$ values are generally lower than α_{GA} values for those groups of layers, with more accentuated differences at low frequencies. A percentage difference up to 45 % may be required from α_{GA} values to obtain $\alpha_{\gamma eq}$ values.

As expected, modeling the acoustic properties of theatre boxes still represent a challenging task in room acoustic simulations because such articulated system of small coupled volumes behave as a group of resonators, return-

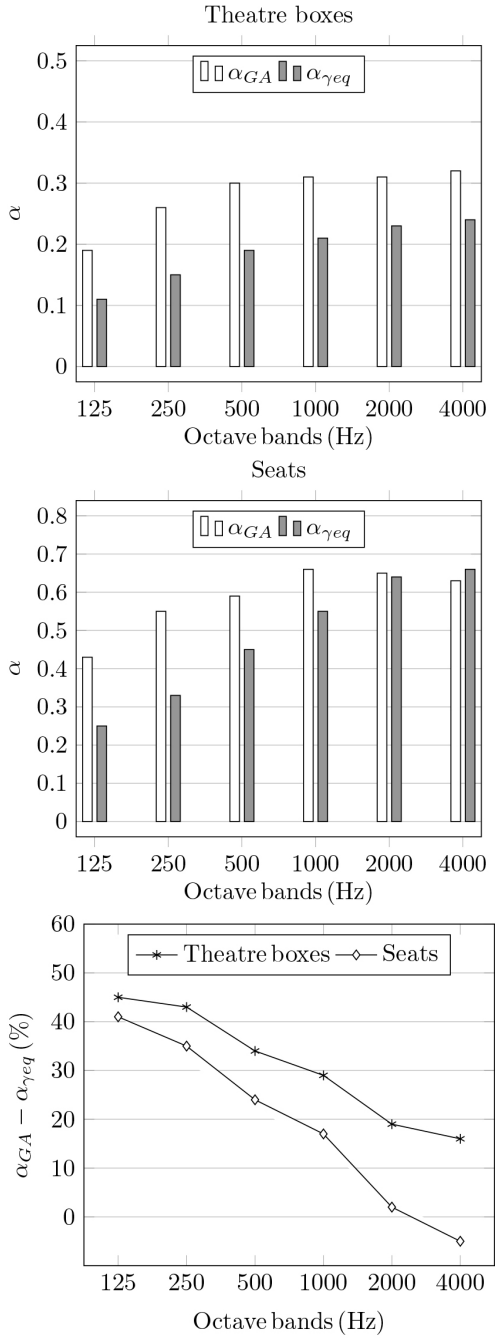

Figure 3: Mean differences between FDTD and GA datasets employed in calibrated models related to the theatre boxes and the seats. In GA calibrations, α_{GA} refer to the energy parameters actually assigned to the surfaces, in FDTD calibrations $\alpha_{\gamma eq}$ values have been re-converted from the acoustic admittances actually used in the simulation.

ing sound energy in the main hall delayed in time [20,25]. Similarly, as the surfaces corresponding to the seat rows are causing edge diffraction, the main theoretical and computational difference between WB and GA methods become more prominent, especially at low frequencies. In fact, the mean difference in percentage is always higher than 30% in the octave bands centered on 125 Hz and 250 Hz whereas it drops for the upper octave bands. In case of seats, it becomes negative at 4000 Hz probably due to the numerical dispersion errors at high frequencies [47].

5. CONCLUSIONS

The main concerns about using WB methods have been primarily caused by high computational cost and the implementation of frequency-dependent wall impedances. Such issues, which represented significant obstacles up to the most recent decades, have been increasingly overcome in the last years. In this work, current opportunities in WB large-scale room acoustics applications have been exploited, with a special focus on the input data assigned to the boundaries. The FDTD model chosen for this study was tested in four different large non-trivial halls for wider frequency ranges compared to the usual wave-based applications. The FDTD calibration of the 3D virtual models was developed keeping the parallel standard GA procedure by way of comparison and the experimental data as reference point. At the end of the calibration processes, the analysis of input datasets used in the two simulation approaches has been provided in terms of differences between α_{GA} and the equivalent $\alpha_{\gamma eq}$ derived from complex-valued admittances actually employed in FDTD calibrations. The outcomes highlight a significant overestimation of α_{GA} compared to $\alpha_{\gamma eq}$ with accentuated discrepancies at low frequencies, in line with previous findings. Materials employed for calibrating the coupled-volume virtual opera houses, including 3D models, experimental results, and boundary conditions are freely available in online repositories [48,49].

6. REFERENCES

[1] A. Krokstad, S. Strom, and S. Sørsdal, "Calculating the acoustical room response by the use of a ray tracing technique," *Journal of Sound and Vibration*, vol. 8, no. 1, pp. 118–125, 1968.

[2] M. R. Schroeder and K. Kuttruff, "On frequency response curves in rooms. comparison of experimental,

theoretical, and monte carlo results for the average frequency spacing between maxima," *The Journal of the Acoustical Society of America*, vol. 34, no. 1, pp. 76–80, 1962.

[3] L. Savioja and U. P. Svensson, "Overview of geometrical room acoustic modeling techniques," *The Journal of the Acoustical Society of America*, vol. 138, no. 2, pp. 708–730, 2015.

[4] *ISO 354:2003 Acoustics — Measurement of sound absorption in a reverberation room*.

[5] *ASTM C423:2022 Standard Test Method for Sound Absorption and Sound Absorption Coefficients by the Reverberation Room Method*.

[6] M. Vorländer, *Auralization*. Springer, 2020.

[7] T. J. Cox and P. D'antonio, *Acoustic absorbers and diffusers: theory, design and application*. Crc Press, 2009.

[8] D. Botteldooren, "Finite-difference time-domain simulation of low-frequency room acoustic problems," *The Journal of the Acoustical Society of America*, vol. 98, no. 6, pp. 3302–3308, 1995.

[9] L. Savioja, "Real-time 3d finite-difference time-domain simulation of low and mid frequency room acoustics," in *Proc. 13th Conf. on Digital Audio Effects (DAFx)*, vol. 1, p. 75, 2010.

[10] C. J. Webb and S. Bilbao, "Computing room acoustics with cuda-3d fdtd schemes with boundary losses and viscosity," in *2011 IEEE International Conference on Acoustics, Speech and Signal Processing (ICASSP)*, pp. 317–320, IEEE, 2011.

[11] M. Aretz, *Combined wave and ray based room acoustic simulations of small rooms*, vol. 12. Logos Verlag Berlin GmbH, 2012.

[12] F. Pind, A. P. Engsig-Karup, C.-H. Jeong, J. S. Hesthaven, M. S. Mejling, and J. Strømann-Andersen, "Time domain room acoustic simulations using the spectral element method," *The Journal of the Acoustical Society of America*, vol. 145, no. 6, pp. 3299–3310, 2019.

[13] B. Mondet, J. Brunskog, C.-H. Jeong, and J. H. Rindel, "From absorption to impedance: Enhancing boundary conditions in room acoustic simulations," *Applied Acoustics*, vol. 157, p. 106884, 2020.

[14] C.-H. Jeong and J. Brunskog, "The equivalent incidence angle for porous absorbers backed by a hard surface," *The Journal of the Acoustical Society of America*, vol. 134, no. 6, pp. 4590–4598, 2013.

[15] H. Kuttruff, *Room acoustics*. Crc Press, 2016.

[16] H. Wang, J. Yang, and M. Hornikx, "Frequency-dependent transmission boundary condition in the acoustic time-domain nodal discontinuous galerkin model," *Applied Acoustics*, vol. 164, p. 107280, 2020.

[17] C. K. Tam and L. Auriault, "Time-domain impedance boundary conditions for computational aeroacoustics," *AIAA journal*, vol. 34, no. 5, pp. 917–923, 1996.

[18] G. Fratoni, B. Hamilton, and D. D'Orazio, "Feasibility of a finite-difference time-domain model in large-scale acoustic simulations," *The Journal of the Acoustical Society of America*, vol. 152, no. 1, pp. 330–341, 2022.

[19] G. Fratoni, "Standardization of procedures and calculation models for the numerical simulation of acoustics of enclosed spaces.," Ph.D. Dissertation. University of Bologna, Italy, 2021.

[20] S.-i. Sato, S. Wang, Y. Zhao, S. Wu, H. Sun, N. Prodi, C. Visentin, and R. Pompoli, "Effects of acoustic and visual stimuli on subjective preferences for different seating positions in an italian style theater," *Acta Acustica united with Acustica*, vol. 98, no. 5, pp. 749–759, 2012.

[21] J. H. Rindel, "Room acoustic modelling techniques: A comparison of a scale model and a computer model for a new opera theatre," *Building Acoustics*, vol. 18, no. 3-4, pp. 259–280, 2011.

[22] *ISO 3382-1:2009 Acoustics — Measurement of room acoustic parameters*.

[23] R. Pompoli and N. Prodi, "Guidelines for acoustical measurements inside historical opera houses: procedures and validation," *Journal of sound and vibration*, vol. 232, no. 1, pp. 281–301, 2000.

[24] T. Hidaka and L. L. Beranek, "Objective and subjective evaluations of twenty-three opera houses in europe, japan, and the americas," *The Journal of the Acoustical Society of America*, vol. 107, no. 1, pp. 368–383, 2000.

[25] N. Prodi, R. Pompoli, F. Martellotta, and S.-i. Sato, "Acoustics of italian historical opera houses," *The Journal of the Acoustical Society of America*, vol. 138, no. 2, pp. 769–781, 2015.

[26] D. D'Orazio, "Italian-style opera houses: A historical review," *Applied Sciences*, vol. 10, no. 13, p. 4613, 2020.

[27] D. D'Orazio, A. Rovigatti, and M. Garai, "The proscenium of opera houses as a disappeared intangible heritage: a virtual reconstruction of the 1840s original design of the alighieri theatre in ravenna," in *Acoustics*, vol. 1, pp. 694–710, Multidisciplinary Digital Publishing Institute, 2019.

[28] D. D'Orazio, G. Fratoni, and M. Garai, "Enhancing the strength of symphonic orchestra in an opera house," *Applied Acoustics*, vol. 170, p. 107532, 2020.

[29] D. D'Orazio, G. Fratoni, A. Rovigatti, and M. Garai, "A virtual orchestra to qualify the acoustics of historical opera houses," *Building Acoustics*, p. 1351010X20912501, 2020.

[30] F. Brinkmann, L. Aspöck, D. Ackermann, S. Lepa, M. Vorländer, and S. Weinzierl, "A round robin on room acoustical simulation and auralization," *The Journal of the Acoustical Society of America*, vol. 145, no. 4, pp. 2746–2760, 2019.

[31] S. Siltanen, T. Lokki, L. Savioja, and C. Lynge Christensen, "Geometry reduction in room acoustics modeling," *Acta Acustica united with Acustica*, vol. 94, no. 3, pp. 410–418, 2008.

[32] C.-H. Jeong, G. Marbjerg, and J. Brunskog, "Uncertainty of input data for room acoustic simulations," in *Proc. of bi-annual Baltic-Nordic Acoustic Meeting*, 2016.

[33] M. Vorländer, "Computer simulations in room acoustics: Concepts and uncertainties," *The Journal of the Acoustical Society of America*, vol. 133, no. 3, pp. 1203–1213, 2013.

[34] S. Bilbao, "Modeling of complex geometries and boundary conditions in finite difference/finite volume time domain room acoustics simulation," *IEEE Transactions on Audio, Speech, and Language Processing*, vol. 21, no. 7, pp. 1524–1533, 2013.

[35] S. D. Bilbao, *Numerical sound synthesis*. Wiley Online Library, 2009.

[36] B. Hamilton, "Finite difference and finite volume methods for wave-based modelling of room acoustics.," Ph.D. Dissertation. University of Edinburgh, UK, 2016.

[37] B. Hamilton and C. J. Webb, "Room acoustics modelling using gpu-accelerated finite difference and finite volume methods on a face-centered cubic grid," *Proc. Digital Audio Effects (DAFx), Maynooth, Ireland*, pp. 336–343, 2013.

[38] G. M. Naylor, "Odeon—another hybrid room acoustical model," *Applied Acoustics*, vol. 38, no. 2-4, pp. 131–143, 1993.

[39] C. L. Christensen and J. H. Rindel, "A new scattering method that combines roughness and diffraction effects," in *Forum Acousticum, Budapest, Hungary*, pp. 344–352, 2005.

[40] Y. H. Kim, H. M. Lee, C. K. Seo, and J. Y. Jeon, "Investigating the absorption characteristics of open ceilings in multi-purpose halls using a 1: 25 scale model," *Applied acoustics*, vol. 71, no. 5, pp. 473–478, 2010.

[41] B. N. Postma and B. F. Katz, "Perceptive and objective evaluation of calibrated room acoustic simulation auralizations," *The Journal of the Acoustical Society of America*, vol. 140, no. 6, pp. 4326–4337, 2016.

[42] B. N. Postma and B. F. Katz, "Creation and calibration method of acoustical models for historic virtual reality auralizations," *Virtual Reality*, vol. 19, pp. 161–180, 2015.

[43] S. Bilbao, B. Hamilton, J. Botts, and L. Savioja, "Finite volume time domain room acoustics simulation under general impedance boundary conditions," *IEEE/ACM Transactions on Audio, Speech, and Language Processing*, vol. 24, no. 1, pp. 161–173, 2015.

[44] M. Vercammen, *On the revision of ISO 354, measurement of the sound absorption in the reverberation room*. Universitätsbibliothek der RWTH Aachen, 2019.

[45] Y. H. Kim, "Prediction of sound absorption properties of audience chairs for music performing spaces using computer simulations," *Applied Acoustics*, vol. 197, p. 108928, 2022.

[46] A. Pilch, "Optimization-based method for the calibration of geometrical acoustic models," *Applied Acoustics*, vol. 170, p. 107495, 2020.

[47] B. Hamilton, C. Webb, N. Fletcher, and S. Bilbao, "Finite difference room acoustics simulation with general impedance boundaries and viscothermal losses in air: Parallel implementation on multiple gpus," in *Proc. Int. Symp. Musical Room Acoust*, 2016.

[48] G. Fratoni, "Materials for calibrating four complex virtual environments through acoustic simulations," doi.org/10.17632/y7xnv6xg5s.

[49] G. Fratoni, "Materials for calibrating coupled-volume virtual opera houses through acoustic simulations," doi.org/10.17632/kgj4h7ddcd.